PNAS RESEARCH ARTICLE | MICROBIOLOGY OPEN ACCESS

A recombinant VSV-vectored vaccine rapidly protects nonhuman primates against lethal Nipah virus disease

Stephanie L. Foster[a,b,1], Courtney Woolsey[a,b,1], Viktoriya Borisevich[a,b], Krystle N. Agans[a,b], Abhishek N. Prasad[a,b], Daniel J. Deer[a,b], Joan B. Geisbert[a,b], Natalie S. Dobias[a,b], Karla A. Fenton[a,b], Robert W. Cross[a,b], and Thomas W. Geisbert[a,b,2]

Edited by Diane Griffin, Johns Hopkins University, Baltimore, MD; received January 3, 2022; accepted February 2, 2022

Nipah virus (NiV) is an emerging highly lethal zoonotic disease that, like SARS-CoV-2, can be transmitted via respiratory droplets. Single-injection vaccines that rapidly control NiV outbreaks are needed. To assess the ability of a vaccine to induce fast-acting protection, we immunized African green monkeys with a recombinant vesicular stomatitis virus (VSV) expressing the Bangladesh strain glycoprotein (NiV_BG) of NiV (rVSV-ΔG-NiV_BG). Monkeys were challenged 3 or 7 d later with a lethal dose of NiV_B. All monkeys vaccinated with rVSV-ΔG-NiV_BG 7 d prior to NiV_B exposure were protected from lethal disease, while 67% of animals vaccinated 3 d before NiV_B challenge survived. Vaccine protection correlated with natural killer cell and cytotoxic T cell transcriptional signatures, whereas lethality was linked to sustained interferon signaling. NiV G-specific antibodies in vaccinated survivors corroborated additional transcriptomic findings, supporting activation of humoral immunity. This study demonstrates that rVSV-based vaccines may have utility in rapidly protecting humans against NiV infection.

Nipah virus | henipavirus | vaccine | rVSV-NiV | recombinant vesicular stomatitis virus

Nearly 20 y ago, Nipah virus (NiV) emerged and was shown to be a previously unknown paramyxovirus, now classified along with Hendra virus (HeV) and Cedar virus within the *Henipavirus* genus (1). NiV causes febrile encephalitis and severe respiratory disease in humans with a case-fatality rate (CFR) as high as 100% in some outbreaks (2). Pteropid fruit bats have been identified as the reservoir for NiV in nature, although pigs served as an amplifying host during the first outbreak of NiV in Malaysia (3). Additionally, there are numerous other mammalian species that are susceptible to NiV infection (4).

NiV is classified as a biosafety level-4 pathogen because of the high mortality rates associated with infection, the lack of effective medical countermeasures, and the ease of transmission. In addition to causing morbidity and mortality as a naturally acquired infection, NiV is classified as a Category C priority pathogen and transboundary select agent by several US government agencies (5). NiV and henipaviral diseases are included on the World Health Organization's Blueprint List of Priority Pathogens and NiV is included on the Coalition for Epidemic Preparedness Innovations priority list (5). Because of the global pandemic of COVID-19, there is heightened concern regarding respiratory pathogens. In 2020, the US Centers for Disease Control and Prevention recommended that NiV be added to the list of Tier 1 Select Agents (6). Indeed, NiV causes lethal infection in nonhuman primates (NHPs) when delivered by small-particle aerosol (7–9). The characteristics of NiV enhancing its global pandemic potential are as follows: humans are susceptible; NiV is capable of person-to-person transmission; it is an RNA virus with potential to mutate; and if a human-adapted strain were to infect communities in South Asia, high population densities and global interconnectedness would rapidly spread the infection (10).

Outbreaks of NiV occur almost annually in Bangladesh and India. In 2018, 23 cases and 21 deaths of NiV disease were reported in the state of Kerala, India (91% CFR); in 2019, an isolated case was reported in the same region; in 2020, six cases of NiV disease were reported; and more recently in September 2021, the virus claimed the life of a 12-y-old boy in Kerala (11–13). Genetic analysis has identified at least two strains of NiV responsible for outbreaks in different geographical areas (14, 15). The Malaysia strain (NiV_M) caused the initial outbreak of NiV from 1998 to 1999 in Malaysia and Singapore, in which over 270 people were infected with an ∼40% CFR (16), and caused an additional 2014 outbreak in the Philippines with a CFR of ∼52% (17). The Bangladesh strain (NiV_B), however, has caused repeated outbreaks in Bangladesh and India between 2001 and 2018 (16, 18, 19). Outbreaks of NiV_B have higher CFRs, averaging about 75% with human-to-human transmission also observed (20). The

Significance

Concern has increased about the pandemic potential of Nipah virus (NiV). Similar to SARS-CoV-2, NiV is an RNA virus that is transmitted by respiratory droplets. There are currently no NiV vaccines licensed for human use. While several preventive vaccines have shown promise in protecting animals against lethal NiV disease, most studies have assessed protection 1 mo after vaccination. However, in order to contain and control outbreaks, vaccines that can rapidly confer protection in days rather than months are needed. Here, we show that a recombinant vesicular stomatitis virus vector expressing the NiV glycoprotein can completely protect monkeys vaccinated 7 d prior to NiV exposure and 67% of animals vaccinated 3 d before NiV challenge.

Author affiliations: [a]Galveston National Laboratory, University of Texas Medical Branch, Galveston, TX 77555-0610; and [b]Department of Microbiology and Immunology, University of Texas Medical Branch, Galveston, TX 77555-0610

Author contributions: R.W.C. and T.W.G. designed research; S.L.F., C.W., V.B., K.N.A., A.N.P., D.J.D., J.B.G., N.S.D., K.A.F., R.W.C., and T.W.G. performed research; S.L.F., C.W., V.B., K.N.A., A.N.P., D.J.D., J.B.G., N.S.D., K.A.F., and T.W.G. analyzed data; and S.L.F., C.W., K.A.F., and T.W.G. wrote the paper.

Competing interest statement: S.L.F., R.W.C., and T.W.G. are listed on a provisional US patent application for henipavirus vaccines (US Serial No. 63/248,055).

This article is a PNAS Direct Submission.

[1]S.L.F. and C.W. contributed equally to this work.

[2]To whom correspondence may be addressed. Email: twgeisbe@utmb.edu.

This article contains supporting information online at http://www.pnas.org/lookup/suppl/doi:10.1073/pnas.2200065119/-/DCSupplemental.

Published March 14, 2022.

observations that these two strains reportedly display differences in CFRs and human-to-human transmission are interesting, as there is 91.8% nucleotide homology between the genomes (15). Importantly, we have developed NHP models for both NiV_M (21) and NiV_B (22) and showed that NiV_B is more pathogenic in African green monkeys (AGMs) than NiV_M under identical experimental conditions (22). We also showed that treatments that protect AGMs against NiV_M have a shorter therapeutic window against NiV_B, demonstrating the importance of any medical countermeasure to protect against the more virulent NiV_B (22).

Currently, there are no vaccines licensed for the prevention of NiV disease. To date, at least eight experimental preventive candidate vaccines against henipaviruses have been evaluated in preclinical animal models. Vaccinia and canarypox viruses encoding NiV_M F or NiV_M G have shown protection against NiV_M in hamsters and pigs (23, 24); a recombinant adenovirus-associated virus vaccine expressing NiV_M G completely protected hamsters against homologous NiV_M challenge (25); a recombinant chimpanzee adenovirus vaccine expressing NiV_B G completely protected hamsters against exposure to NiV_B and NiV_M (26); and a virus-like particle-based NiV vaccine protected hamsters against homologous NiV_M challenge (27). Other vaccine candidates include a recombinant measles virus vector expressing NiV_M G that demonstrated some efficacy in the NiV_M AGM model (28), a messenger RNA (mRNA) vaccine encoding HeV G that partially protected hamsters against NiV_M (29), and a recombinant subunit vaccine based on the HeV G protein (HeV sG) that completely protected cats and ferrets against lethal NiV_M infection (30, 31). This vaccine was also shown to be efficacious in AGM models of NiV_M and NiV_B infection (32, 33). Several groups have developed recombinant vesicular stomatitis virus (rVSV)-based NiV vaccines. A replication-competent rVSV-based vaccine encoding NiV_M G was highly efficacious in hamsters (34) and provided protection even when administered 1 d before exposure to NiV_M (35). This vaccine also protected AGMs from NiV_M disease 1 mo after a single intramuscular administration (36). However, this vaccine relies on inclusion of the *Zaire ebolavirus* (EBOV) glycoprotein for replication and has not yet been tested against NiV_B. Single-cycle replication rVSVs have been developed against NiV and have shown strong immunogenicity, as high neutralizing antibody titers were generated in mice vaccinated with an rVSV expressing either NiV_M F or NiV_M G (37). These vaccine vectors were shown to provide homologous protection in the hamster model of NiV_M infection (38). We recently developed alternative single-cycle rVSV vaccine vectors expressing either the NiV_B F or NiV_B G proteins along with green fluorescent protein (GFP) (39). These vaccines were evaluated 28 d after a single-dose vaccination in ferret and AGM models and were shown to completely protect ferrets and AGMs from lethal NiV_M challenge (39); AGMs were also protected against lethal NiV_B disease (40).

While the majority of candidate NiV vaccine platforms demonstrated a robust immune response in laboratory animals, most of these vaccines required multiple injections to confer protective efficacy. Few studies have shown complete protection in the "gold standard" AGM model. In the context of NiV, which is indigenous to regions of Asia and a potential agent of bioterrorism, a single-injection vaccine is preferable. In the case of preventing natural infections, multiple-dose vaccines are both too costly and not practical in developing countries. In the case of a deliberate release or a natural outbreak of NiV, there would be little time for deployment of a vaccine that requires multiple injections over a prolonged period. Thus, for most real-world applications a vaccine against NiV requires a single immunization providing rapid protection.

Most previous preclinical vaccine studies have assessed protective efficacy against NiV approximately 4 to 5 wk after the final vaccination. An NiV vaccine that confers efficacy in days instead of weeks is needed to control outbreaks most effectively. The rVSV vectors that we previously developed and employed to protect AGMs against the highly pathogenic NiV_B contain GFP, which is not suitable for advanced development. Therefore, we first constructed and rescued an rVSV-based single-cycle vector expressing NiV_BG (rVSV-ΔG-NiV_BG). We then assessed the ability of the rVSVΔG-NiV_BG vaccine to induce protective immunity in the uniformly lethal AGM model of NiV_B at 3 or 7 d after vaccination.

Results

Recovery of rVSV-ΔG-NiV_BG. As a fluorescent marker would be an obstacle to clinical trials and future licensure, we created a single-cycle VSV G-complemented rVSV-vectored NiV_B G vaccine lacking GFP (*SI Appendix*, Fig. S1). Quantification of the virus by conventional plaque assay on G-complemented BHK cells indicated a stock titer of 4.25×10^8 plaque-forming units (PFU)/mL, confirming the vaccine grows to similarly high titers in cell culture as other rVSV-based vaccine vectors (41).

To confirm our rVSV vaccine expresses NiV_B G immunogen, an immunofluorescence assay was performed on infected Vero 76 and BHK-21 clone WI-2 cells (*SI Appendix*, Fig. S2). Unlike mock-infected cells, abundant expression of NiV_B G protein was detected in cells infected with rVSV-ΔG-NiV_B G. While the subcellular localization of the NiV_B G protein was not confirmed, similar expression in infected permeabilized and nonpermeabilized cells was observed, suggesting NiV_B G protein is capable of trafficking to the cell surface for immune recognition.

Vaccination and Challenge of AGMs. Following recovery and characterization of the rVSV-ΔG-NiV_BG vaccine, we tested its ability to rapidly protect AGMs from lethal challenge with NiV_B. The AGM model faithfully recapitulates human NiV disease, and challenge with 5×10^5 PFU of NiV_B is uniformly lethal (22). Specifically, we aimed to determine whether shorter periods between vaccination and challenge were sufficient to yield protection, as an earlier version of the vaccine fully protected monkeys from NiV_B when given ∼1 mo prior to virus exposure.

Two studies with nine AGMs each (six specifically vaccinated with rVSV-ΔG-NiV_B G, three vector control subjects) were conducted to accomplish this objective. Animals were vaccinated either 7 d (study 1) (Fig. 1*A*) or 3 d (study 2) (Fig. 1*B*) prior to challenge. Each subject received 1×10^7 PFU of rVSV-ΔG-NiV_BG vaccine or 1×10^7 PFU of a rVSV-ΔG-EBOV 76 nonspecific vector control. All AGMs were subsequently challenged with 5×10^5 PFU of NiV_B by combined intranasal and intratracheal routes.

For study 1, 100% of rVSV-ΔG-NiV_BG-vaccinated subjects survived to the 35-d postinfection (DPI) study endpoint, whereas AGMs receiving the nonspecific rVSV vaccine succumbed to NiV disease 7 to 9 DPI (Fig. 2*A*). For the second study, 67% of animals receiving rVSV-ΔG-NiV_BG survived to the study endpoint (Fig. 2*B*). Thus, the rVSV-ΔG-NiV_BG

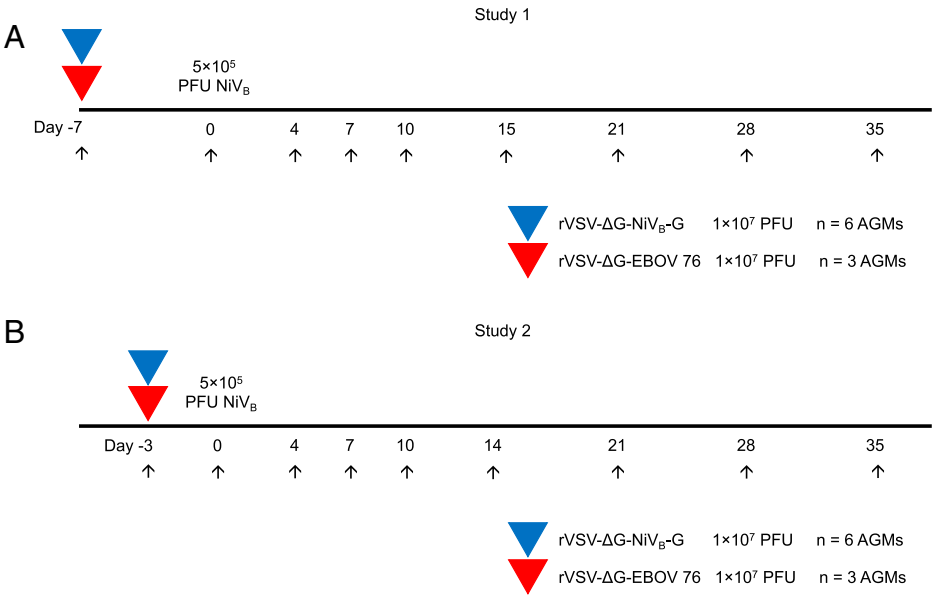

Fig. 1. Study designs for experimental NiV_B challenge studies in AGMs. Experimental design for (*A*) study 1, in which AGMs were vaccinated 7 d prior to challenge with NiV_B, and (*B*) study 2, in which AGMs were vaccinated 3 d prior to challenge. The red triangle indicates vaccination with the nonspecific rVSV-ΔG-EBOV 76 control vector, while the blue triangle denotes vaccination with the rVSV-ΔG-NiV_BG vector developed for these studies. Study days relative to challenge with 5×10^5 PFU of NiV_B are shown below the horizontal black line, with days of blood collection indicated with arrows.

vaccine was highly effective even when administered as soon as 3 d prior to exposure.

AGMs that received the rVSV-ΔG-NiV_BG vaccine 7 d prior to challenge (study 1) did not exhibit any clinical signs other than decreased appetite throughout the study (*SI Appendix*, Table S1). Clinical pathology was minimal, although some subjects had transient increases in C-reactive protein (CRP) (V7-2, V7-5, V7-6), indicating inflammatory processes. Within this cohort, various hematological cell counts were also outside baseline values. Conversely, all animals receiving the nonspecific vaccine 7 d prior to challenge developed dyspnea and depression prior to reaching euthanasia criteria. Increased respiration rates, a hallmark of NiV disease, were evident in vector control AGMs prior to euthanasia (*SI Appendix*, Fig. S3*A*). These findings indicate an overall respiratory decline in these subjects. All surviving specifically vaccinated animals had stable respiration rates over the course of the study. The vector control cohort also had decreased levels of white blood cells, lymphocytes, and thrombocytes, suggesting immune suppression in association with hemorrhagic disease. Vector controls also had elevated concentrations of neutrophils, monocytes, and CRP.

Similar to study 1, animals in study 2 receiving the nonspecific rVSV-ΔG-EBOV 76 vector control ($n = 3$) developed respiratory and systemic signs consistent with NiV disease, such as increased respiration rates, tachypnea, dyspnea, and depression (*SI Appendix*, Fig. S3*B* and Table S2). All vector controls reached euthanasia criteria by 7 to 8 DPI. Unlike study 1, in which all specifically immunized animals appeared healthy, specifically vaccinated AGMs in study 2 developed clinical signs consistent with NiV disease. Two of the animals vaccinated with rVSV-ΔG-NiV_BG met euthanasia criteria at 6 DPI (V3-1, V3-2), which is in line with the typical time-to-death (TTD) for this model. Therefore, specific vaccination did not appear to protract the disease course or delay death. The four remaining subjects in this group (V3-3, V3-4, V3-5, V3-6) developed transient respiratory signs (*SI Appendix*, Fig. S3*B* and Table S2) and showed transient CRP increases but recovered and survived to the 35 DPI study endpoint. Regardless of disposition (survivor/fatal) or vaccine administered, all subjects developed thrombocytopenia or lymphopenia over the course of the study. An increase in inflammatory cells (monocytes and granulocytes) was also a prominent finding in all animals in study 2. Generally, clinical pathology and disease severity was less severe in vaccinated survivors. Clinical pathology values returned to normal by ∼10 DPI in these subjects.

Pathology of Vaccinated AGMs Challenged with NiV_B. Pathology was consistent with NiV infection in the six unvaccinated control AGMs (C7-1, C7-2, C7-3, C3-1, C3-2, C3-3); similar lesions were noted in the two specifically vaccinated AGMs vaccinated 3 d before NiV_B challenge and euthanized 6 DPI (V3-1, V3-2) (Fig. 3 *A*–*E*). Gross lesions present in AGMs that

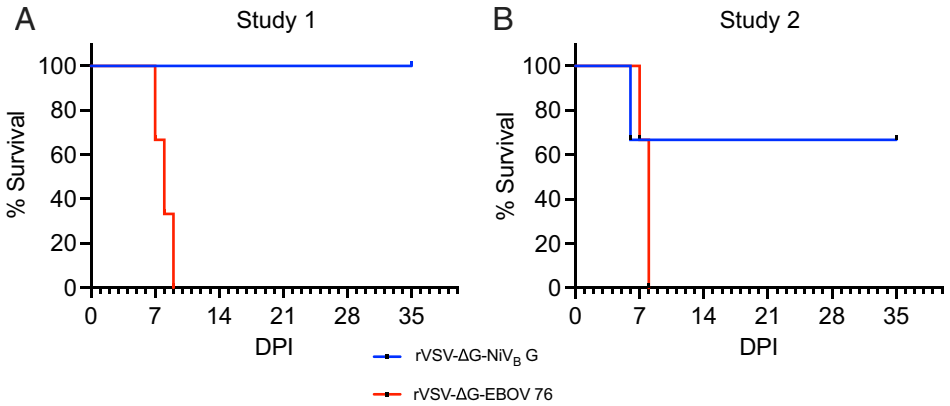

Fig. 2. Survival curves following challenge of AGMs with NiV_B. Kaplan–Meier survival curves for AGMs vaccinated with rVSV-ΔG-NiV_BG (blue line) or a nonspecific control (rVSV-ΔG-EBOV 76) (red line) at (*A*) 7 d (study 1) or (*B*) 3 d (study 2) prior to challenge with NiV_B.

succumbed to infection included hepatic congestion, splenomegaly, hemorrhagic interstitial pneumonia, and pleural effusion. Histologic lesions correlated with the gross pathology. Loss of normal splenic architecture with fibrin deposition within the red pulp, lymphocytolysis with numerous multinucleated cells in the white pulp, expansion of pulmonary alveolar septae with inflammatory infiltrates, increased alveolar macrophages, and flooding of alveolar spaces with fibrin, edema, and hemorrhage were noted in fatal cases, consistent with NiV infection (Fig. 3 *B* and *D*). Additionally, colocalized immunohistochemistry labeling for anti-NiV nucleoprotein (N) antigen was present in mononuclear cells, multinucleated cells, and endothelium within the spleen and lung (Fig. 3 *C* and *E*). No histologic lesions or labeling by immunohistochemistry was noted in the examined sections of brain from fatal cases. The remaining four AGMs vaccinated 3 d prior to NiV_B exposure that survived (V3-3, V3-4, V3-5, V3-6) and all six AGMs vaccinated 7 d before NiV_B challenge (V7-1, V7-2, V7-3, V7-4, V7-5, V7-6) failed to display gross or histologic lesions consistent with NiV infection (Fig. 3 *F*–*O*).

Viral Loads in Vaccinated AGMs Challenged with NiV_B. For study 1, no animals vaccinated with rVSV-ΔG-NiV_B G had detectable viremia by either plaque assay or reverse transcriptase quantitative PCR (qRT-PCR). Conversely, vector controls had detectable viremia (two animals by plaque assay and all three animals by qRT-PCR) shortly prior to being euthanized (Fig. 4 *A* and *B*). For study 2, all specifically and nonspecifically vaccinated fatal AGMs had similar peak viral loads by plaque assay and qRT-PCR, ranging from 1×10^6 to 1×10^8 genome equivalents (GEq) per milliliter for the latter (Fig. 4 *C* and *D*). Additionally, two of the four survivors vaccinated with rVSV-ΔG-NiV_B G developed viremia detectable by qRT-PCR, although viral loads were cleared by 10 DPI (Fig. 4*D*). No virus was detected in these subjects by either method prior to 6 DPI or after 8 DPI

Neutralizing and Anti-NiV_B G Binding Antibody Titers in Vaccinated AGMs. To determine if humoral responses contributed to rapid protection in these studies, we performed 50% plaque reduction neutralization tests ($PRNT_{50}$) and ELISAs to quantify neutralizing and binding antibody titers to NiV, respectively. All survivors in study 1 (animals V7-1 through V7-6) (Fig. 5*A*) and study 2 (animals V3-3 through V3-6) (Fig. 5*B*) developed neutralizing antibodies beginning at 7 DPI. Interestingly, animals in study 2 exhibited higher neutralizing antibody titers than subjects in study 1, suggesting a stronger humoral response may be needed to control infection whenever the vaccine is administered at a shorter interval. None of the vector control nor specifically vaccinated animals that succumbed to NiV disease developed neutralizing antibodies.

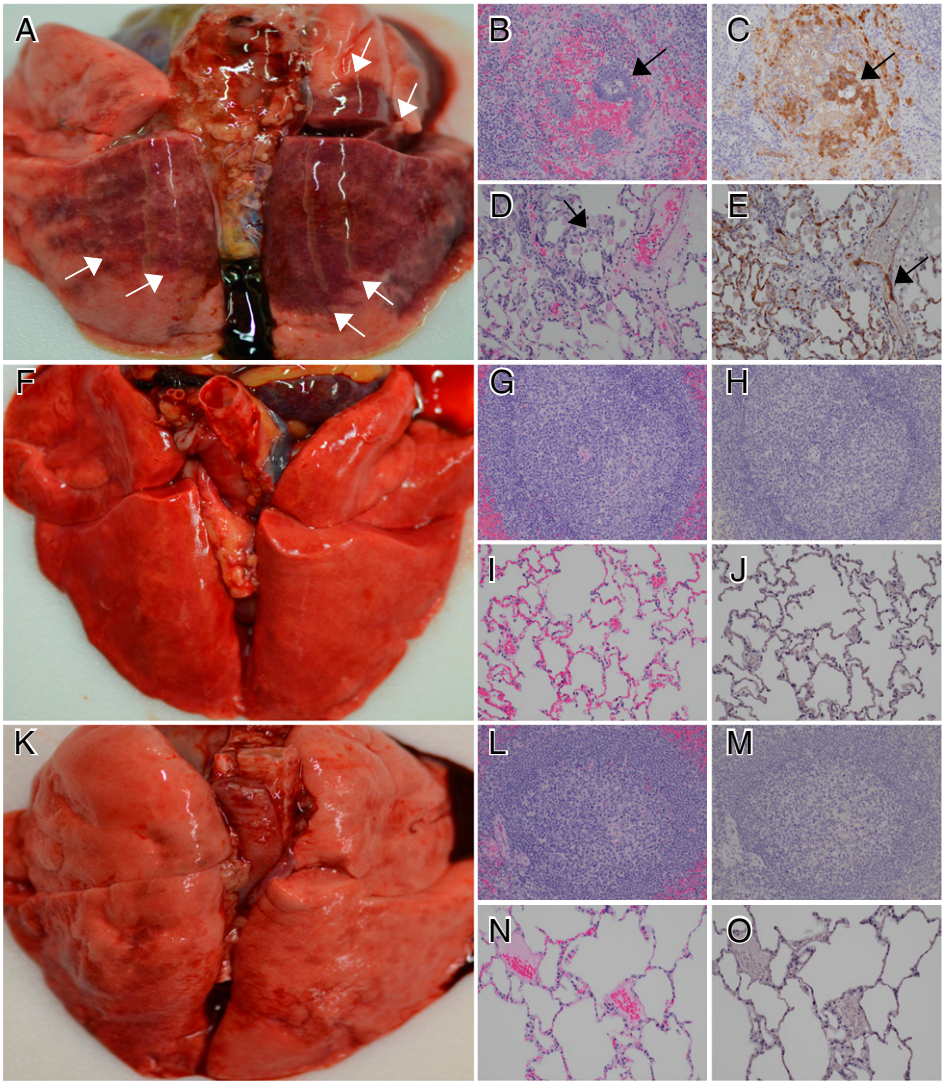

Fig. 3. Pathology lesions in AGMs exposed to NiV_B. Vector control (Subject C7-1). (*A*) Multifocal hemorrhagic interstitial pneumonia (white arrows). (*B*) Loss of normal splenic architecture with lymphocytolysis, hemorrhage, and multinucleated cells (black arrow) in germinal centers. (*C*) IHC^+ immunolabeling (brown) of mononuclear cells and multinucleated cells (black arrow) within the germinal center of the spleen. (*D*) Expansion of alveolar septea with mononuclear inflammatory cells, flooding of alveolar space with edema, hemorrhage, and increased alveolar macrophages (black arrow). (*E*) IHC^+ immunolabeling (brown) of endothelium (black arrow) and alveolar septate of the lung. Pathology representative of AGMs that survived NiV_B infection −7 d (subject V7-6) (*F–J*) and −3 d (subject V3-3) (*K–O*) prior to NiV_B challenge. (*F* and *K*) No gross pulmonary lesions; (*G* and *L*) no splenic histologic lesions; (*H* and *M*) no IHC immunolabeling for anti-NiV N antigen of the spleen; (*I* and *N*) no pulmonary histologic lesions; and (*J* and *O*) no IHC immunolabeling for anti-NiV N antigen of the lung. All photomicrographs taken at 20×.

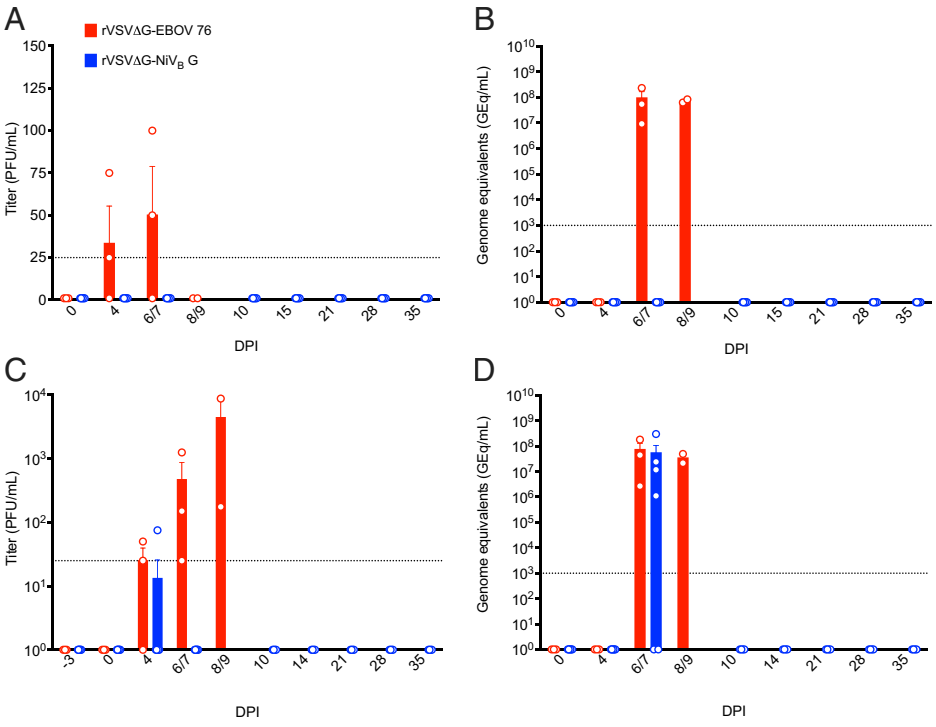

Fig. 4. Viremia in AGMs after challenge with NiV$_B$. Infectious virus isolated from EDTA plasma by plaque assay (*A* and *C*) or viral RNA detected in whole blood by qRT-PCR specific for NiV$_B$ (*B* and *D*) for AGMs challenged with NiV$_B$ 7 d after vaccination (*A* and *B*) or 3 d after vaccination (*C* and *D*). Subjects vaccinated with rVSV-ΔG-EBOV 76 are represented by red circles, and subjects vaccinated with VSV G-complemented rVSV-ΔG-NiV$_B$G are represented by blue circles (bars represent the mean of the values for all members of the group at each timepoint, and error bars represent the SEM). The limit of detection (LOD) for each assay is indicated by a dotted horizontal line. The LOD for the plaque assays is 25 PFU; qRT-PCR values are reported as 1 GEq/mL if they were below the LOD (1,000 copies/mL). EDTA, ethylenediaminetetraacetic acid.

Congruent with the PRNT$_{50}$ results, only specifically vaccinated survivors formed substantial binding antibody titers. Anti-NiV G IgM (Fig. 5*C*) and IgG (Fig. 5*E*) titers were detected as early as 4 DPI in animals vaccinated 7 d prior to challenge, whereas IgM (Fig. 5*D*) and IgG (Fig. 5*F*) were not detected until 6 to 10 DPI in subjects vaccinated 3 d prechallenge. These results suggest that antibodies form as quickly as 10 to 11 d postvaccination with rVSV-ΔG-NiV$_B$G. rVSV-ΔG-NiV$_B$G–vaccinated survivors from study 1 and study 2 developed moderate to robust IgG titers (1:400 to 1:102,400) by 10 DPI (Fig. 5 *E* and *F*). For study 1, IgG titers slightly declined at the 35 DPI convalescent timepoint in survivors (Fig. 5*E*), conjointly with IgM titers for both studies (Fig. 5 *C* and *D*).

Transcriptomics on Fatal and Survivor Whole-Blood Samples. To identify additional correlates of lethality or rVSV-ΔG-NiV$_B$G–mediated protection, we performed transcriptomics on peripheral whole-blood samples collected from AGMs. Dimensional reduction via principal component analysis revealed variation in the datasets was mostly driven by disposition (vaccinated survivor vs. vector control subjects) for the day −7 group (Fig. 6*A*) and DPI (0, 4, 7, 10 [survivors] or the terminal time point in fatal cases) for the day −3 group (Fig. 6*B*). Irrespective of group or DPI, samples clustered similarly at the day of challenge other than one outlier in the day −7 group, illustrating expression changes predominantly resulted after NiV$_B$ challenge.

For the day −7 group (study 1), the topmost highly expressed transcripts (Benjamini-Hochberg [BH]-adjusted $P < 0.05$) in specifically vaccinated versus vector control samples at late disease (10 DPI) were predominantly involved in adaptive immunity (e.g., *CD40LG*, *ITGA4*, *CD96*, *LILRB1*) and T cell signaling (*SH2D1A*, *CD3E*, *CD8A*) (Fig. 6*C*). The two most highly up-regulated transcripts encode the fractalkine receptor (*CX3CR1*) and T cell-specific transcription factor 1 (*TCF7*); among other functions, CX3CR1 participates in natural killer (NK) cell and innate lymphoid cell recruitment/development (42), and TCF7 is involved in T cell differentiation (43). Additional adaptive immunity-related transcripts that did not specifically map to the "adaptive immunity" gene set included *IKZF3* (encodes Ikaros), which regulates B lymphocyte proliferation and differentiation (44), and *IL21* (encodes interleukin 21 cytokine), which is implicated in the formation of germinal centers as well as the generation and maintenance of T follicular helper (Tfh) cells (45).

Down-regulated mRNAs in subjects specifically vaccinated 7 d before challenge at late disease were instead primarily associated with interferon signaling (e.g., *IFIT2*, *GBP1*, *IFIT1*, *MX1*, *OASL*, *IFIT3*) (Fig. 6*D*) or innate immune responses (e.g., *FCAR*, *CLEC4E*, *IL-8*). Transcripts encoding C-X-C motif chemokine ligand 10 (CXCL10), also known as interferon γ-induced protein 10 (IP-10), were also expressed at lower levels in survivors. IP-10 is considered a key regulator in cytokine storm for SARS-CoV-2 and EBOV infections (46, 47). Transient activation of these transcripts was observed at 4 DPI but subsided by 7 DPI, indicating resolution of the acute-phase response in specifically vaccinated subjects. Similarly, transcripts encoding for programmed death ligand 1 (PDL-1), an immune checkpoint protein (48), were also expressed at higher levels at 4 DPI in vaccinated subjects but decreased in expression at later time points.

As incomplete protection was observed in study 2, we next interrogated the immunomes of animals immunized 3 d before NiV$_B$ challenge to determine transcriptional signatures of lethality or survival (Fig. 7*A*). Similar to the study 1 results, specifically vaccinated versus control subjects had higher expression of transcripts enriching to adaptive immunity at 7 DPI and 10 DPI (e.g., *ZAP70*, *KLRC2*, *CD3E*, *LCK*, *CD3D*, *CD247*; BH-adjusted $P < 0.05$). Other transcripts mapping to adaptive immunity included those involved in T cell receptor (TCR) signaling (*CD3E*, *CD3D*, *CD247*, *ZAP70*). Increased expression of *TNFRSF17*, a marker expressed in mature B lymphocytes (49), also pointed to B cell activation. The most highly expressed transcripts in specifically vaccinated AGMs included granzyme A (*GZMA*), granzyme K (*GZMK*),

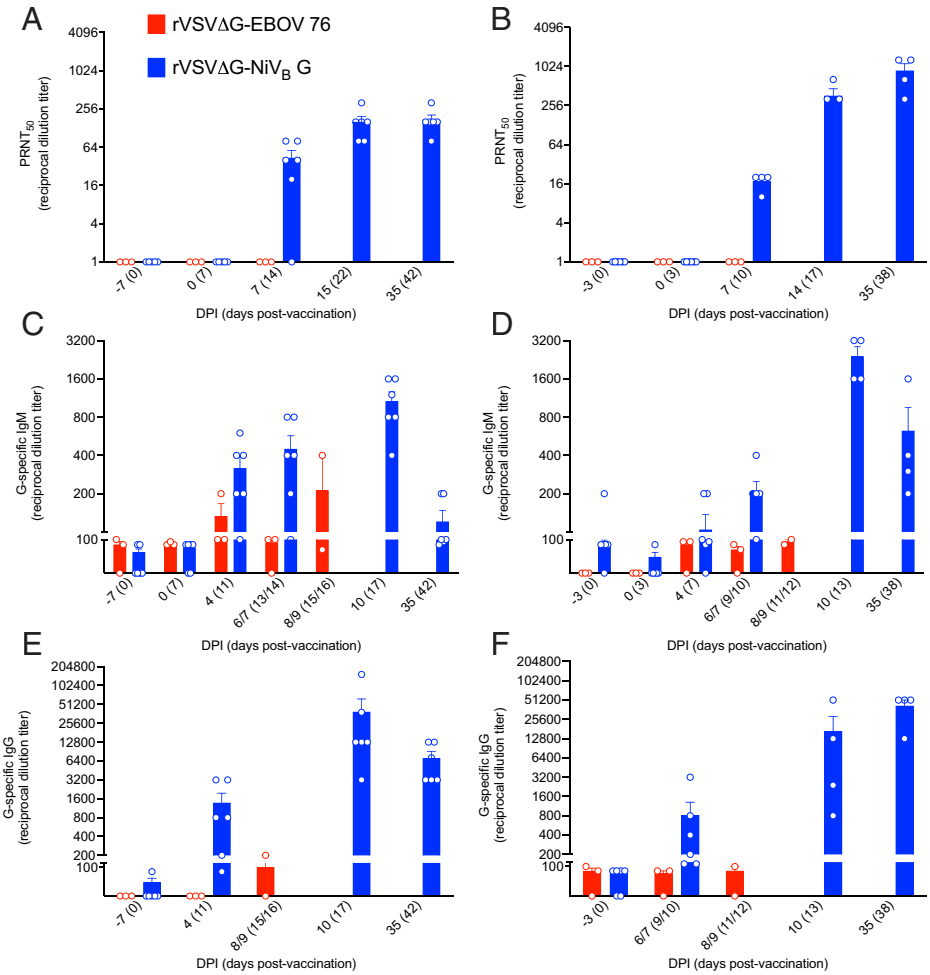

Fig. 5. Neutralizing and anti-NiV$_B$ G binding antibody titers in AGMs. (*A* and *B*) PRNT$_{50}$ values from EDTA plasma, reported as reciprocal dilutions at which plaque counts were reduced by 50% compared to control wells, for animals vaccinated with VSV G-complemented rVSV-ΔG-NiV$_B$G (blue symbols) or rVSV-ΔG-EBOV 76 (nonspecific control) (red symbols) (*A*) 7 d or (*B*) 3 d prior to challenge with NiV$_B$. (*C*–*F*) Reciprocal dilution binding anti-NiV G IgM (*C* and *D*) or IgG (*E* and *F*) titers in subjects vaccinated at −7 d (*C* and *E*) or −3 d (*D* and *F*) postchallenge. Height of the bar graph represents the group mean with SEM at each indicated time point, while open circles represent values for individual subjects. Parentheses denote respective day of vaccination.

granzyme B (*GZMB*), and granulysin (*GNLY*). These mRNAs encode cytoplasmic granules within cytotoxic T cells (CTLs) and NK cells that can induce programmed cell death of infected cells (50). *KLRC2* and *KLRC3* were also more abundantly expressed in specifically vaccinated subjects, and these encode for killer cell lectin receptors that are preferentially expressed on NK cells (51, 52), further supporting NK cells may participate in viral clearance.

Highly expressed mRNAs shared between day −7 and day −3 group vaccinated survivors at late-stage disease included *CD3E*, *NFATC2*, and *ITGA4* (Figs. 6*C* and 7*A*). *CD3E* encodes a component of the TCR (53); *NFATC2* encodes a cytosolic protein that translocates to the nucleus upon TCR stimulation (54); and *ITGA4* encodes Integrin 4α (CD49d), a lymphocyte homing receptor (55). In the fatal group, these molecules were down-regulated at 4 and 7 DPI, indicating they may be associated with rVSV-ΔG-NiV$_B$G–mediated protection (Fig. 7*A*). At 7 DPI and 10 DPI, fatal cases also had lower expression of *CCL5*, *LCK*, *IKBKE*, *CD5*, and *ITGA4*.

For study 2, the most heavily down-regulated transcripts in subjects vaccinated with rVSV-ΔG-NiV$_B$G at late disease mapped to interferon signaling, as evidenced by diminished expression of IFIT transcripts (*IFIT1*, *IFIT2*, *IFIT3*) and other interferon-stimulated genes (*DDX58* [encodes RIG-I], *IFIH1* [encodes MDA-5], *MX1*, *OASL*, *GBP1*, and so forth) at 7 and 10 DPI (Fig. 7*B*). In accordance with study 1, these mRNAs were more robustly expressed at 4 DPI in specifically vaccinated subjects (Figs. 6*D* and 7*B*). Differentially expressed transcripts between fatal and survivor vaccinated samples included *CXCL10* (encodes IP-10) and *FCAR* (encodes Fc fragment of IgA receptor, a transmembrane glycoprotein present on the surface of various myeloid lineage cells) (Fig. 7*B*) (56). These results suggest sustained interferon signaling, inflammation, and myeloid cell recruitment may play a role in the immunopathology of NiV$_B$ disease.

To predict cell-type quantities based on transcriptional signatures, we performed digital cell quantification (DCQ) via nSolver. This analysis demonstrated that survival was associated with increased frequencies of cells involved in adaptive immunity (T cells, CD8 T cells, Th1 cells, cytotoxic cells, and B cells) for both study 1 and study 2, in line with our differential expression results (Fig. 8*A*). Conversely, lethality regardless of time of vaccination correlated with increased neutrophil frequencies, which was corroborated by our hematology data (*SI Appendix*, Tables S1 and S2).

A more in-depth DCQ analysis using CIBERSORT (57) for study 2 (vaccinated 3 d before NiV$_B$ challenge) revealed similar results (*SI Appendix*, Fig. S4). Increased frequencies of plasma cells and CD8 T cells were detected in survivors at 7 and 10 DPI and memory B cells at 10 DPI. A notable finding was that

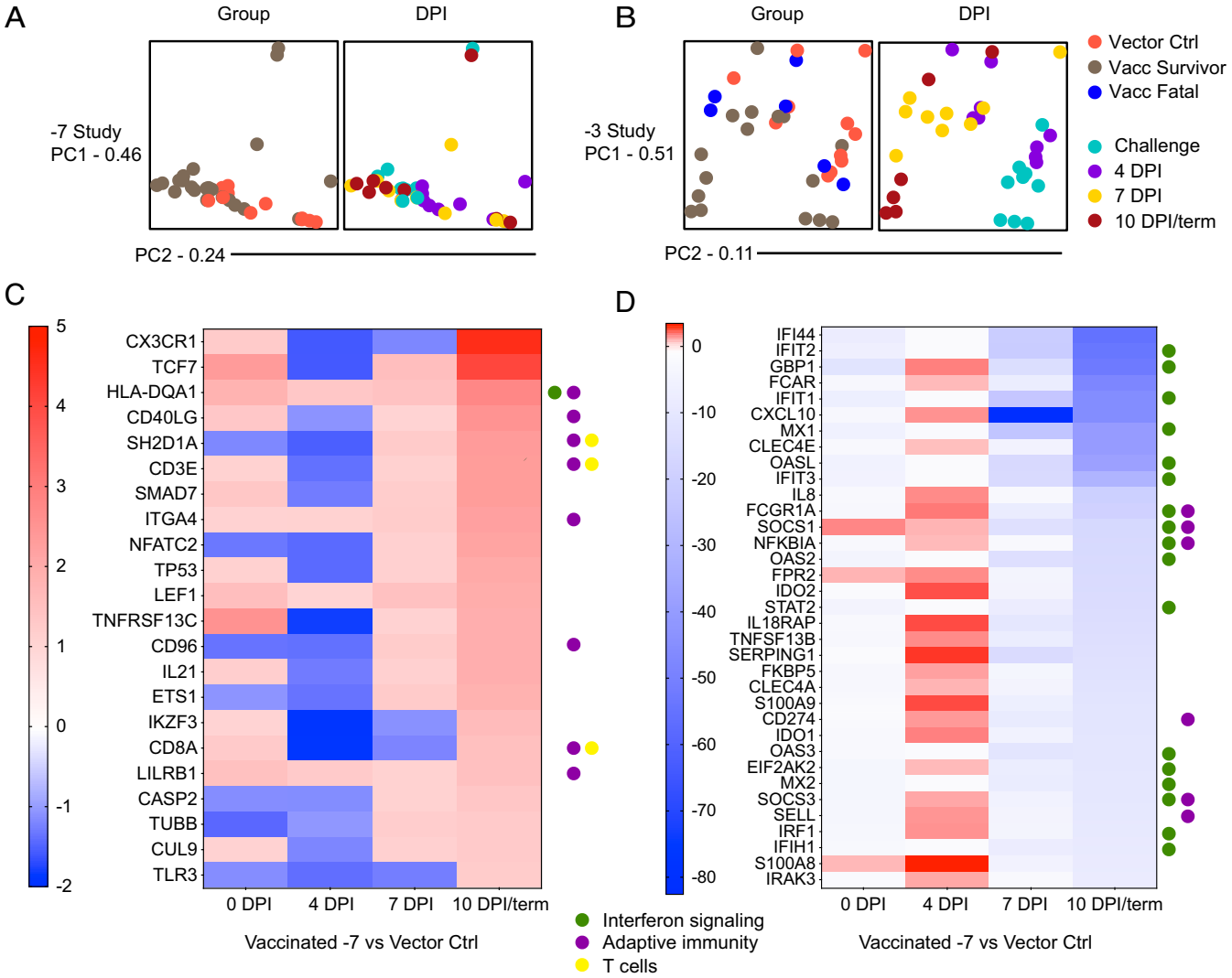

Fig. 6. Transcriptional responses in AGMs after challenge with NiV_B. Principal component analysis based on group (nonspecific vector control, $n = 3$; rVSV-ΔG-NiV_B-G-vaccinated, $n = 6$) and DPI (0, 4, 7, 10 [survivors] or the terminal time point for fatal cases) for study 1 (*A*) or study 2 (*B*). (*C* and *D*) Heatmaps depicting the most highly up-regulated (*C*) or down-regulated (*D*) immunity-specific mRNAs in the −7 vaccinated versus vector control group at late disease (10 DPI; false discovery rate [FDR]-adjusted $P < 0.05$). A BH test was used to derive FDR-adjusted *P* values. Dots indicate transcripts mapping to interferon signaling (green), adaptive immunity (purple), or T cell (yellow) nSolver gene sets. For the heatmaps, red denotes up-regulated transcripts, blue denotes down-regulated transcripts, and white denotes no expression change in vaccinated versus control groups at the indicated time points. Abbreviations: ctrl, control; PC1, principal component 1; PC2, principal component 2; Vacc, vaccinated.

increased frequencies of NK cells (resting), memory B cells, and activated $CD4^+$ memory T cells were found early in infection (4 DPI), suggesting earlier activation of adaptive immunity. Recruitment of these cells corresponded with higher eosinophil and neutrophil frequencies, which again corresponded with our clinical pathology results (*SI Appendix*, Table S2). Lethality corresponded with increased predicted frequencies of naïve B cells, resting $CD4^+$ memory T cells, and $\gamma\delta$ T cells at late disease (10 DPI). In this cohort, monocyte-affiliated transcripts were also more highly expressed at 4 DPI in fatal cases.

Finally, we determined canonical signaling pathways associated with rVSV-ΔG-NiV_BG–mediated protection (Fig. 8*B*). In agreement with our differentially expressed enrichment and DCQ results, survival at 10 DPI was associated with NK cell signaling and activation of cell-mediated immunity, including OX40 signaling, cytotoxic T lymphocyte-mediated apoptosis of target cell, calcium-induced T lymphocyte apoptosis, and T cell receptor signaling pathways. Canonical pathways involved in humoral or adaptive immunity were also up-regulated in survivors including CD40 signaling, April-mediated signaling, CD27 signaling, ICOS-ICOLS signaling in T helper cells, and PKC-theta signaling in T lymphocytes.

Collectively, our targeted transcriptome data indicate that rVSV-ΔG-NiV_BG–mediated vaccination corresponded with activation of adaptive immunity, whereas nonspecific vaccination led to sustained interferon signaling and myeloid cell activation.

Discussion

In summary, we have shown rVSV-ΔG-NiV_BG is a highly effective single-cycle vaccine in AGMs when administered 7 d prior to exposure and partially protective when given at 72 h prechallenge. No overt clinical illness or detectable viremia was observed in subjects vaccinated with rVSV-ΔG-NiV_BG 1 wk before virus challenge. Animals vaccinated 3 d prechallenge developed viremia and clinical signs consistent with NiV_B disease, but these were generally resolved by 10 DPI.

For licensure, rVSV-ΔG-NiV_BG has an ideal profile. First, rVSV-based vaccines are safe and effective, as evidenced by the

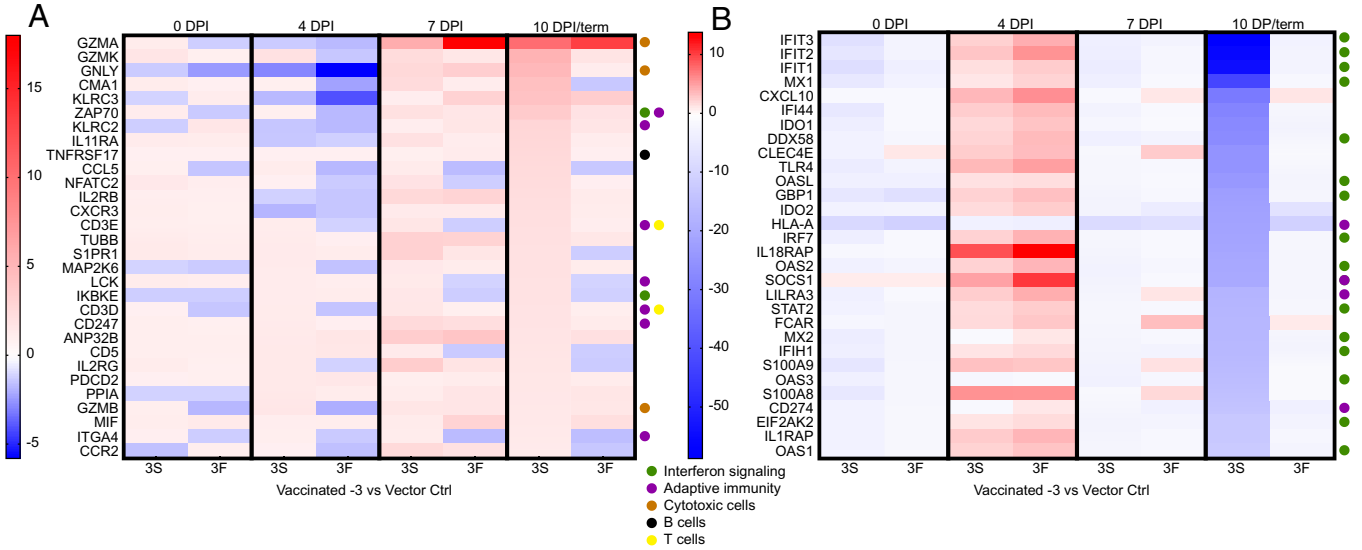

Fig. 7. Differential expression of vaccinated versus control AGM transcripts after challenge with NiV_B. (*A* and *B*) Heatmaps depicting the most highly up-regulated (*A*) or down-regulated (*B*) immunity-specific mRNAs in the −3 vaccinated survivor (3S; $n = 4$) and fatal (3F; $n = 2$) versus vector control ($n = 3$) samples filtered at late disease (10 DPI for survivors or the terminal time point in fatal cases); FDR-adjusted $P < 0.05$. A BH test was used to derive FDR-adjusted P values. Dots indicate transcripts mapping to interferon signaling (green), adaptive immunity (purple), or T cell (yellow), B cell (black), or cytotoxic cell (brown) nSolver gene sets. For the heatmaps, red denotes up-regulated transcripts, blue denotes down-regulated transcripts, and white denotes no expression change in vaccinated versus control groups at the indicated time points. Abbreviations: F3, vaccinated fatal group ($n = 2$) for study 2 (−3 d immunization); S3, vaccinated survivor group ($n = 4$) for study 2 (−3 immunization).

licensure of Ervebo, Merck's rVSV-vectored Ebola vaccine by the US Federal Drug Administration and European Medicines Agency (58). While VSV causes severe disease in cattle, horses, and swine with symptoms similar to foot-and-mouth disease, infection in humans is generally asymptomatic or mild (41). The rVSV-ΔG-NiV_BG vaccine features additional attenuations that enhance its safety profile. It is a single-cycle vector that does not encode the main virulence factor of VSV, VSV G (59); however, since it is complemented with VSV G, the host cell repertoire is expanded due to the inclusion of a more promiscuous receptor. Another safety feature of rVSV-ΔG-NiV_BG is that it encodes only one of the two NiV proteins necessary for viral entry (60).

Late-onset encephalitis and other neurological issues can accompany NiV infection (61). Ensuring these concerns are not exacerbated by administration of rVSV-ΔG-NiV_BG will be important for future development of this vaccine. Our group has previously shown NHPs intrathalamically inoculated with an rVSV-ΔG–based vaccine did not induce neurovirulence, in contrast to wild-type VSV encoding its native glycoprotein (62). It is also encouraging that none of the specifically vaccinated AGM survivors in this study developed neurological signs up to the 35 DPI endpoint. Although rVSV-ΔG-NiV_BG is replication-defective, immunogenicity is retained as evidenced by the rapid development of humoral and cellular responses in AGMs in this study. Preexisting immunity against the vector is an unlikely concern, as there is low VSV seroprevalence in the general population (41), and previous immunization with a Lassa virus rVSV-based vector did not abrogate immunity against EBOV disease following a subsequent rVSV vaccination with an EBOV-based rVSV vaccine in NHPs (63). Other attractive features of the rVSV-ΔG-NiV_BG vaccine include its inability to revert to virulent NiV_B, as it is not an attenuated NiV, and its inability to reassort or integrate into the host genome (41). Lastly, rVSV-ΔG-NiV_BG grows to high titers exceeding 1×10^8 PFU/mL within 24 h, so large-scale manufacturing within a short timeframe is achievable.

The most extensively studied and advanced NiV vaccine candidate is HeV sG (64). A phase 1 clinical trial to assess the safety of an alum-adjuvanted HeV sG vaccine in human volunteers is currently underway (Clinical Trial #NCT04199169). In preclinical trials, HeV sG was shown to be safe, immunogenic, and highly effective at preventing NiV disease in ferrets, cats, and AGMs (30–33). Previous experiments evaluating HeV sG as a vaccine candidate employed two doses, with the second dose given at least 20 d prior to NiV challenge. Conversely, the rVSV-ΔG-NiV_BG vaccine does not require an adjuvant or boost. For outbreak intervention, a single-dose vaccine providing fast-acting protection is essential. A more recent report evaluating HeV sG vaccine as a single dose showed the vaccine was partially protective in AGMs against NiV disease when given 7 to 14 d prior to challenge (33). While these results are promising, a larger cohort is needed to better interpret these results, as only three to four subjects were used per time point in this experiment. Shorter vaccination intervals have not been tested. In our study, a single 1×10^7 PFU dose of rVSV-ΔG-NiV_BG protected 100% or 67% of AGMs from lethality when administered 7 or 3 d before exposure to a uniformly lethal dose of NiV_B, respectively. Given its higher demonstrated efficacy, continued development of the rVSV-ΔG-NiV_B G vaccine is a worthwhile endeavor.

Mechanisms of rapid rVSV-mediated immunity are ill-defined. A previous study showed that 100% of hamsters vaccinated with a replicating rVSV-vectored NiV vaccine 1 d prior to challenge survived a NiV_M challenge, whereas partial protection was observed in groups vaccinated on the day of challenge (67% survival; four of six subjects) or 1 d after challenge (17% survival; one of six subjects) (35). As this vaccination window is insufficient to mount an adaptive response, the authors attributed this protection to viral interference or activation of innate immunity. Corroborating this hypothesis, hamsters vaccinated with a nonspecific vector also exhibited partial protection, with 50% survival (three of six subjects) observed at 1 d before exposure and 17% survival (one of six subjects) observed on the day of challenge. For our study, a similar nonspecific control did not confer protection or even delay the TTD. All control AGMs vaccinated with rVSV-ΔG-EBOV 76 succumbed to NiV disease 7 to 9 DPI. Therefore, survival in this case was

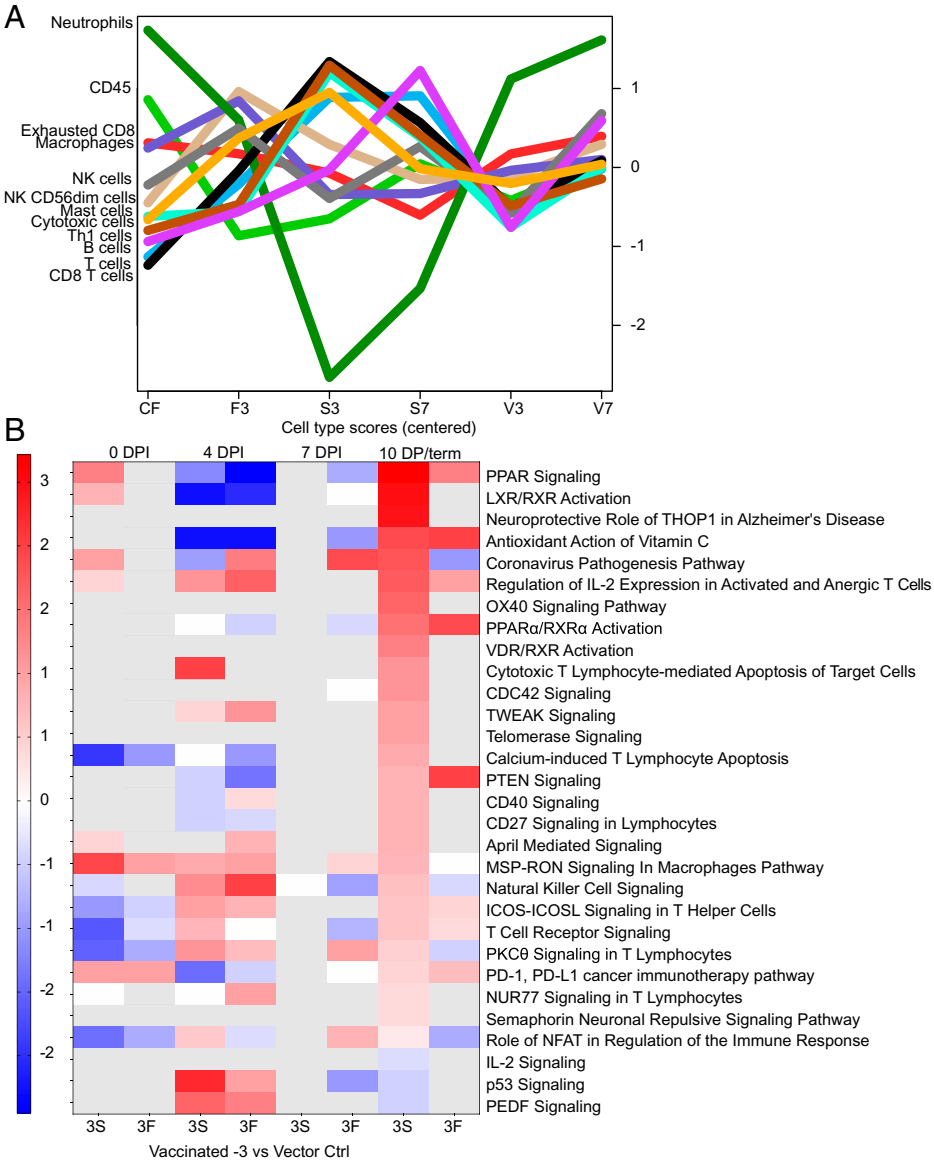

Fig. 8. Predicted cell subset frequencies and canonical signaling pathways in AGMs challenged with NiV_B. (*A*) Trend plot depicting overall nSolver derived cell-type quantities in control and vaccinated (fatal or survivor) cohorts. (*B*) Heatmap depicting the most significant canonical signaling pathways in −3 d vaccinated survivor (3S; $n = 4$) and nonsurvivor (3F; $n = 2$) samples versus vector control ($n = 3$) samples at late disease (FDR-adjusted $P < 0.05$). Red denotes up-regulated pathways; blue denotes down-regulated pathways; white denotes no change in expression; gray denotes lack of sufficient transcripts mapping to specific pathway. Abbreviations: CF, unvaccinated control fatal group ($n = 3$); F3, vaccinated fatal group ($n = 2$) for study 2 (−3 d immunization); S3, vaccinated survivor group ($n = 4$) for study 2 (−3 immunization); S7, vaccinated survivor group ($n = 6$) for study 1 (−7 d immunization); V3, vector control group ($n = 3$) for study 2 (−3 d immunization); V7, vector control group ($n = 3$) for study 1 (−7 d immunization).

dependent on antigen-specific responses and not solely based on innate or rVSV-specific immunity. This is further supported by the development of humoral responses along with the expression of CTL-associated transcripts in vaccinated survivors prior to the typical TTD in this animal model. This discrepancy could be attributed to several factors, including: 1) the time of vaccination (an immunization closer to the day of NiV exposure may afford a greater degree of protection); 2) NiV_B is a more pathogenic variant than NiV_M (22); 3) the briefer disease course of NiV_B does not allow ample time for the host to mount an adaptive response; and 4) compared to hamsters, AGMs serve as a more stringent animal model for evaluating medical countermeasures. One caveat to this study is that the nonspecific vector used as a control in these studies is fully replicative, unlike rVSV-ΔG-NiV_BG. However, we argue that this control served as a more robust comparison for evaluating the efficacy of rVSV-ΔG-NiV_BG as the replicating vaccine should have elicited equal or greater innate and rVSV-specific responses.

All surviving animals developed neutralizing antibodies to NiV_B, although for AGMs vaccinated 3 d before exposure, these antibodies were not detectable until the window during which nonsurvivors were euthanized. Substantial IgM and IgG titers were absent in fatal cases, regardless of the vaccine administered, whereas anti-NiV G binding antibodies formed ∼10 to 11 d post-vaccination, or 4 or 7 DPI for AGM survivors vaccinated at 7 or at 3 d prechallenge, respectively. These findings indicate non-neutralizing antibody-mediated mechanisms such as antibody-dependent cell-mediated cytotoxicity may mediate rVSV-elicited protection. Enrichment of transcripts showed evidence of activation and recruitment of NK cells and cytotoxic lymphocyte degranulation in vaccinated survivors, lending credence to this hypothesis. Although the involvement of NK cells in host resistance to NiV disease remains largely unexplored, other studies have demonstrated the importance of NK cells in rVSV-mediated protection against EBOV (65) and Marburg virus (66).

To define the survivor phenotype, we compared survivor and fatal samples in AGMs vaccinated with rVSV-ΔG-NiV_BG 3 d prior to NiV_B exposure. Our transcriptomic analyses indicated both humoral and cellular responses may act in concert to mediate protection. At late disease, higher predicted frequencies of plasma cells, memory B cells, and $CD8^+$ T cells were observed in survivor versus fatal cases. Specific pathways associated with T cell-mediated immunity in vaccinated survivors included nuclear factor of activated T cells (NFAT), CD40, OX40, and protein kinase

C (PKC-θ) signaling, which are all activated following the productive engagement of T cells by antigen-presenting cells (54, 67–69). Fatal cases had lower expression of *CCL5*, *LCK*, *CD5*, and *ITGA4* transcripts, all of which are implicated in adaptive immunity (70–73). These molecules can serve as prognostic indicators along with CXCL10 (IP-10) and FCAR (glycoprotein present on the surface of myeloid lineage cells, such as neutrophils, monocytes, macrophages, and eosinophils), which were expressed at higher levels in vaccinated nonsurvivors. IP-10 is a chemoattractant involved in inflammation and neurotoxicity (74), which is associated with the pathogenesis of NiV disease (75). This protein was abundantly expressed in the brain of human patients who succumbed to lethal NiV infection during an outbreak in Malaysia, indicating its potential role in neuroinflammation. Sustained interferon signaling and activation of innate immunity responses were also prominent findings in fatal cases, similar to another study investigating natural immunity to henipaviruses in NHPs (76). Natural resistance of cynomolgus macaques to henipavirus infection involved many transcriptional factors we also identified in this study (e.g., *CD5*, *CD3E*, *CCL5*, *GZMB*, *CX3CR1*). Similarly, lethality corresponded with expression of IP-10 and interferon-stimulated genes. Further characterization is needed to confirm our transcriptional results are also reflected at the protein level. Follow up experiments should include flow cytometry and single-cell transcriptomics to fully analyze the contribution of NK cells and humoral and cellular arms of adaptive immunity.

Based on this study, the rVSV vector system appears to accelerate activation of innate and adaptive immunity but expression of NiV-specific antigen is still necessary to elicit protection. As other vaccine platforms have used NiV G as an immunogen but required multiple doses or were only partially effective, antigen presentation and a rVSV-specific antiviral response are both likely important components for defense against henipaviruses. Although a previous study showed NHPs immunized with rVSV-NiV_B-GFP vaccines expressing F, G, or F and G at ∼1 mo prior to NiV_B challenge all survived (40), this study is unique in showing rapid onset of protection with rVSV-based vaccines. Our results indicate presentation of NiV G alone is sufficient to mount a swift protective response.

In conclusion, rVSV-ΔG-NiV_BG is a safe, immunogenic, and effective vaccine that protected AGMs from a high dose of NiV_B given shortly after vaccination. These studies are an encouraging first step in showing the safety and potential efficacy of this vaccine in an outbreak scenario. Future studies are needed to identify the minimum dose needed for efficacy, as well as to define the durability of vaccine-induced immune responses. Manufacturing of clinical grade vaccine lots is also needed to push this vaccine toward licensure. With the recent issues concerning the stability and transport of COVID-19 vaccines, it will be useful to explore whether rVSV-based NiV vaccines can be formulated to be stable for long-term storage at 2 to 8 °C or at least −20 °C. A fast-acting and effective vaccine is urgently needed for NiV, which still causes outbreaks in India and Bangladesh nearly every year with high CFRs. The rVSV-ΔG-NiV_BG vaccine will be an invaluable tool in controlling this deadly pathogen.

Materials and Methods

Cloning of pVSV-ΔG-NiV_BG. The pVSV-ΔG-NiV_B G plasmid was constructed by Gibson assembly. Additional detailed materials and methods are provided in the *SI Appendix*.

Recovery of rVSV-ΔG-NiV_BG. The VSV G-complemented rVSV-ΔG-NiVB G vaccine construct was recovered using a modified previously described protocol (77). Additional detailed methods are provided in the *SI Appendix*.

Characterization of rVSV-ΔG-NiV_BG Vaccine. The rVSV-ΔG-NiV_BG vaccine was characterized by sequencing as described in the *SI Appendix*.

The vaccine was tested and found to be negative for mycoplasma and endotoxin contamination.

Immunofluorescence Assay. An immunofluorescence assay was used to check for expression of NiV_B G in rVSV-ΔG-NiV_B G-infected cells. Additional detailed methods and reagents are provided in the *SI Appendix*.

Challenge Virus. The isolate of NiV_B used in the study (200401066) was obtained from a fatal human case during the outbreak in Rajbari, Bangladesh in 2004. Additional information is provided in the *SI Appendix*.

NHP Vaccination and Challenge. For the first study, nine healthy, adult AGMs were randomized into a group of six experimental animals and a group of three control animals. The six experimental animals were specifically vaccinated by intramuscular injection of 1×10^7 PFU of rVSV-ΔG-NiV_BG, and control animals were vaccinated by intramuscular injection of 1×10^7 PFU of a nonspecific rVSVΔG-EBOV-GP vaccine (78). All nine AGMs were exposed 7 d after vaccination to 5×10^5 PFU of NiV_B, with the dose being equally divided between intratracheal and the intranasal routes. For the second study, nine healthy, adult AGMs were randomized into a group of six experimental animals and a group of three control animals. The six experimental animals were specifically vaccinated by intramuscular injection of 1×10^7 PFU of rVSV-ΔG-NiV_BG, and control animals were vaccinated by intramuscular injection of 1×10^7 PFU of a nonspecific rVSVΔG-EBOV-GP vaccine. All AGMs were exposed 3 d after vaccination to 5×10^5 PFU of NiV_B with the dose being equally divided between the intratracheal and the intranasal routes. Additional information is provided in the *SI Appendix*.

The AGMs were monitored daily and scored for disease progression. The University of Texas Medical Branch Institutional Animal Care and Use Committee approved our internal NiV humane endpoint scoring sheet. The University of Texas Medical Branch facilities used in this work are accredited by the Association for Assessment and Accreditation of Laboratory Animal Care International and adhere to principles specified in the eighth edition of the *Guide for the Care and Use of Laboratory Animals*, National Research Council (79).

Hematology and Serum Biochemistry. Blood collected in tubes containing EDTA was analyzed using a Vetscan HM5 laser based hematologic analyzer (Zoetis). Additional detailed methods are provided in the *SI Appendix*.

RNA Isolation from NiV_B-Infected AGMs. On specified procedure days, 100 μL of blood was added to 600 μL of AVL viral lysis buffer (Qiagen) for RNA extraction. For tissues, ∼100 mg was stored in 1 mL RNAlater (Qiagen) for 7 d for stabilization. RNAlater was completely removed, and tissues were homogenized in 600 μL RLT buffer (Qiagen) in a 2 mL cryovial using a Tissue Lyser (Qiagen) and ceramic beads. Additional detailed methods are provided in the *SI Appendix*.

Quantification of Viral Load. Viral loads of RNA from blood or tissues were quantitatively assessed using qRT-PCR and primers/probe targeting the N gene and intergenic region between N and P of NiV_B. Probe sequences were 6FAM-5′CGTCACACATCAGCTCTGACAA-3′-6TAMRA for NiV_B (Life Technologies), as described previously (76).

Virus titration was performed by plaque assay using Vero 76 cells (ATCC CRL-1587) from all plasma samples, as previously described (22). Additional detailed methods and reagents are provided in the *SI Appendix*.

ELISA. Sera collected at the indicated time points were tested for total anti-NiV IgG and IgM antibodies by ELISA using monkey species specific kits (#NIV-015 and #NIV-020) obtained from a commercial vendor (Alpha Diagnostic International) following the manufacturer's recommendations.

Plaque Reduction Neutralization Test. Neutralization titers were calculated by determining the dilution of serum that reduced 50% of plaques ($PRNT_{50}$). We incubated a standard 100 PFU amount of NiV_B with twofold serial dilutions of serum samples in DMEM for 1 h. The virus-serum mixture was then used to inoculate Vero 76 cells for 30 minutes. Cells were overlaid with 2× MEM agar medium, incubated for 2 to 3 d, and plaques were counted after 24 h of 5% neutral red staining.

Transcriptomics. NHPV2_Immunology reporter and capture probesets (Nanostring Technologies) were hybridized with ~5 μL of blood RNA at 65 °C for ~24 h, as previously described (80). A full list of probes detected for each sample group along with log fold-changes and *P* values is featured in Dataset S1. Additional detailed methods are provided in the *SI Appendix*. We used CIBERSORT web-based deconvolution software for our cell type predictions (57).

Histology. Tissue sections were processed for histological staining. Detailed methods and reagents are described in the *SI Appendix*.

Statistics and Reproducibility. Indicated statistical tests were performed using Prism 9 (GraphPad). All data are derived from two experiments.

Data Availability. All study data are included in the main text and supporting information. NanoString transcriptomic data are provided in Dataset S1.

ACKNOWLEDGMENTS. We thank the University of Texas Medical Branch Animal Resource Center for husbandry support of laboratory animals; Kevin Melody for assistance with the animal studies; and Chad Mire for technical expertise and assistance in recovery of the rVSV-ΔG-NiV$_B$G vaccine. Opinions, interpretations, conclusions, and recommendations are those of the authors and are not necessarily endorsed by the University of Texas Medical Branch. This study was supported by the US Army Medical Research Acquisition Activity contract W81XWH1910028 (to T.W.G.) and the US Department of Health and Human Services, NIH Grant UC7AI094660 for biosafety level-4 operations support of the Galveston National Laboratory.

1. B. Rima *et al.*; Ictv Report Consortium, ICTV virus taxonomy profile: *Paramyxoviridae*. *J. Gen. Virol.* **100**, 1593–1594 (2019).
2. B. S. P. Ang, T. C. C. Lim, L. Wang, Nipah virus infection. *J. Clin. Microbiol.* **56**, e01875–e01817 (2018).
3. S. A. Rahman *et al.*; Henipavirus Ecology Research Group, Risk factors for Nipah virus infection among pteropid bats, Peninsular Malaysia. *Emerg. Infect. Dis.* **19**, 51–60 (2013).
4. E. de Wit, V. J. Munster, Animal models of disease shed light on Nipah virus pathogenesis and transmission. *J. Pathol.* **235**, 196–205 (2015).
5. R. Gómez Román *et al.*, Medical countermeasures against henipaviruses: A review and public health perspective. *Lancet Infect. Dis.* **22**, e13–e27 (2022).
6. CDC/USDA, Federal Select Agent Program, HHS and USDA Select Agents and Toxins 7CFR Part 331, 9 CFR Part 121, and 42 CFR Part 73 (2021). https://www.selectagents.gov/sat/list.htm?CDC_AA_refVal=https%3A%2F%2Fwww.selectagents.gov%2FSelectAgentsandToxinsList.html. Accessed 9 December 2021.
7. D. A. Hammoud *et al.*, Aerosol exposure to intermediate size Nipah virus particles induces neurological disease in African green monkeys. *PLoS Negl. Trop. Dis.* **12**, e0006978 (2018).
8. Y. Cong *et al.*, Loss in lung volume and changes in the immune response demonstrate disease progression in African green monkeys infected by small-particle aerosol and intratracheal exposure to Nipah virus. *PLoS Negl. Trop. Dis.* **11**, e0005532 (2017).
9. A. N. Prasad *et al.*, A lethal aerosol exposure model of Nipah virus strain Bangladesh in African green monkeys. *J. Infect. Dis.* **221**, S431–S435 (2020).
10. S. P. Luby, The pandemic potential of Nipah virus. *Antiviral Res.* **100**, 38–43 (2013).
11. WHO, Outbreak of Nipah virus encephalitis in the Kerala state of India (01 Jun 2018). (2021) https://www.who.int/southeastasia/outbreaks-and-emergencies/health-emergency-information-risk-assessment/surveillance-and-risk-assessment/nipah-virus-outbreak-in-kerala. Accessed 10 December 2021.
12. WHO, Nipah virus disease–India (17 Sep 2021). (2021) https://www.who.int/emergencies/disease-outbreak-news/item/nipah-virus-disease-india. Accessed 10 December 2021.
13. V. Soman Pillai, G. Krishna, M. Valiya Veettil, Nipah virus: Past outbreaks and future containment. *Viruses* **12**, 465 (2020).
14. K. B. Chua *et al.*, Nipah virus: A recently emergent deadly paramyxovirus. *Science* **288**, 1432–1435 (2000).
15. B. H. Harcourt *et al.*, Genetic characterization of Nipah virus, Bangladesh, 2004. *Emerg. Infect. Dis.* **11**, 1594–1597 (2005).
16. V. Sharma, S. Kaushik, R. Kumar, J. P. Yadav, S. Kaushik, Emerging trends of Nipah virus: A review. *Rev. Med. Virol.* **29**, e2010 (2019).
17. P. K. G. Ching *et al.*, Outbreak of henipavirus infection, Philippines, 2014. *Emerg. Infect. Dis.* **21**, 328–331 (2015).
18. M. K. Lo *et al.*, Characterization of Nipah virus from outbreaks in Bangladesh, 2008–2010. *Emerg. Infect. Dis.* **18**, 248–255 (2012).
19. G. Arunkumar *et al.*; Nipah Investigators People and Health Study Group, Outbreak investigation of Nipah virus disease in Kerala, India, 2018. *J. Infect. Dis.* **219**, 1867–1878 (2019).
20. E. S. Gurley *et al.*, Person-to-person transmission of Nipah virus in a Bangladeshi community. *Emerg. Infect. Dis.* **13**, 1031–1037 (2007).
21. T. W. Geisbert *et al.*, Development of an acute and highly pathogenic nonhuman primate model of Nipah virus infection. *PLoS One* **5**, e10690 (2010).
22. C. E. Mire *et al.*, Pathogenic differences between Nipah virus Bangladesh and Malaysia strains in primates: Implications for antibody therapy. *Sci. Rep.* **6**, 30916 (2016).
23. V. Guillaume *et al.*, Nipah virus: Vaccination and passive protection studies in a hamster model. *J. Virol.* **78**, 834–840 (2004).
24. H. M. Weingartl *et al.*, Recombinant Nipah virus vaccines protect pigs against challenge. *J. Virol.* **80**, 7929–7938 (2006).
25. A. Ploquin *et al.*, Protection against henipavirus infection by use of recombinant adeno-associated virus-vector vaccines. *J. Infect. Dis.* **207**, 469–478 (2013).
26. N. van Doremalen *et al.*, A single-dose ChAdOx1-vectored vaccine provides complete protection against Nipah Bangladesh and Malaysia in Syrian golden hamsters. *PLoS Negl. Trop. Dis.* **13**, e0007462 (2019).
27. P. Walpita *et al.*, A VLP-based vaccine provides complete protection against Nipah virus challenge following multiple-dose or single-dose vaccination schedules in a hamster model. *NPJ Vaccines* **2**, 21 (2017).
28. M. Yoneda *et al.*, Recombinant measles virus vaccine expressing the Nipah virus glycoprotein protects against lethal Nipah virus challenge. *PLoS One* **8**, e58414 (2013).
29. M. K. Lo *et al.*, Evaluation of a single-dose nucleoside-modified messenger RNA vaccine encoding Hendra Virus-soluble glycoprotein against lethal Nipah virus challenge in Syrian hamsters. *J. Infect. Dis.* **221**, S493–S498 (2020).
30. B. A. Mungall *et al.*, Feline model of acute Nipah virus infection and protection with a soluble glycoprotein-based subunit vaccine. *J. Virol.* **80**, 12293–12302 (2006).
31. J. A. Pallister *et al.*, Vaccination of ferrets with a recombinant G glycoprotein subunit vaccine provides protection against Nipah virus disease for over 12 months. *Virol. J.* **10**, 237 (2013).
32. K. N. Bossart *et al.*, A Hendra virus G glycoprotein subunit vaccine protects African green monkeys from Nipah virus challenge. *Sci. Transl. Med.* **4**, 146ra107–146ra141 (2012).
33. T. W. Geisbert *et al.*, A single dose investigational subunit vaccine for human use against Nipah virus and Hendra virus. *NPJ Vaccines* **6**, 23 (2021).
34. B. L. DeBuysscher, D. Scott, A. Marzi, J. Prescott, H. Feldmann, Single-dose live-attenuated Nipah virus vaccines confer complete protection by eliciting antibodies directed against surface glycoproteins. *Vaccine* **32**, 2637–2644 (2014).
35. B. L. DeBuysscher, D. Scott, T. Thomas, H. Feldmann, J. Prescott, Peri-exposure protection against Nipah virus disease using a single-dose recombinant vesicular stomatitis virus-based vaccine. *NPJ Vaccines* **1**, 16002 (2016).
36. J. Prescott *et al.*, Single-dose live-attenuated vesicular stomatitis virus-based vaccine protects African green monkeys from Nipah virus disease. *Vaccine* **33**, 2823–2829 (2015).
37. A. Chattopadhyay, J. K. Rose, Complementing defective viruses that express separate paramyxovirus glycoproteins provide a new vaccine vector approach. *J. Virol.* **85**, 2004–2011 (2011).
38. M. K. Lo *et al.*, Single-dose replication-defective VSV-based Nipah virus vaccines provide protection from lethal challenge in Syrian hamsters. *Antiviral Res.* **101**, 26–29 (2014).
39. C. E. Mire *et al.*, Single injection recombinant vesicular stomatitis virus vaccines protect ferrets against lethal Nipah virus disease. *Virol. J.* **10**, 353 (2013).
40. C. E. Mire *et al.*, Use of single-injection recombinant vesicular stomatitis virus vaccine to protect nonhuman primates against lethal Nipah virus disease. *Emerg. Infect. Dis.* **25**, 1144–1152 (2019).
41. A. Roberts, L. Buonocore, R. Price, J. Forman, J. K. Rose, Attenuated vesicular stomatitis viruses as vaccine vectors. *J. Virol.* **73**, 3723–3732 (1999).
42. M. Nishimura *et al.*, Dual functions of fractalkine/CX3C ligand 1 in trafficking of perforin+/granzyme B+ cytotoxic effector lymphocytes that are defined by CX3CR1 expression. *J. Immunol.* **168**, 6173–6180 (2002).
43. D. Pais Ferreira *et al.*, Central memory CD8$^+$ T cells derive from stem-like Tcf7^{hi} effector cells in the absence of cytotoxic differentiation. *Immunity* **53**, 985–1000 (2020).
44. B. Heizmann, P. Kastner, S. Chan, The Ikaros family in lymphocyte development. *Curr. Opin. Immunol.* **51**, 14–23 (2018).
45. J. J. O'Shea, M. Gadina, R. M. Siegel, "Cytokines and cytokine receptors" in *Clinical Immunology, Principles and Practic.* R. R. Rich *et al.*, Eds. (Elsevier, 2019), pp. 127–155.
46. N. Vaninov, In the eye of the COVID-19 cytokine storm. *Nat. Rev. Immunol.* **20**, 277 (2020).
47. A. K. McElroy *et al.*, Biomarker correlates of survival in pediatric patients with Ebola virus disease. *Emerg. Infect. Dis.* **20**, 1683–1690 (2014).
48. R. Makuku, N. Khalili, S. Razi, M. Keshavarz-Fathi, N. Rezaei, Current and future perspectives of PD-1/PDL-1 blockade in cancer immunotherapy. *J. Immunol. Res.* **2021**, 6661406 (2021).
49. N. Shah, A. Chari, E. Scott, K. Mezzi, S. Z. Usmani, B-cell maturation antigen (BCMA) in multiple myeloma: Rationale for targeting and current therapeutic approaches. *Leukemia* **34**, 985–1005 (2020).
50. I. Voskoboinik, J. C. Whisstock, J. A. Trapani, Perforin and granzymes: Function, dysfunction and human pathology. *Nat. Rev. Immunol.* **15**, 388–400 (2015).
51. D. R. Ram *et al.*, Tracking KLRC2 (NKG2C)+ memory-like NK cells in SIV+ and rhCMV+ rhesus macaques. *PLoS Pathog.* **14**, e1007104 (2018).
52. L. G. Hidalgo, G. Einecke, K. Allanach, P. F. Halloran, The transcriptome of human cytotoxic T cells: Similarities and disparities among allostimulated CD4(+) CTL, CD8(+) CTL and NK cells. *Am. J. Transplant.* **8**, 627–636 (2008).
53. W. Wu *et al.*, Multiple signaling roles of CD3ε and its application in CAR-T cell therapy. *Cell* **182**, 855–871 (2020).
54. S. L. Peng, A. J. Gerth, A. M. Ranger, L. H. Glimcher, NFATc1 and NFATc2 together control both T and B cell activation and differentiation. *Immunity* **14**, 13–20 (2001).
55. S. Glatigny, R. Duhen, C. Arbelaez, S. Kumari, E. Bettelli, Integrin alpha L controls the homing of regulatory T cells during CNS autoimmunity in the absence of integrin alpha 4. *Sci. Rep.* **5**, 7834 (2015).
56. R. Mladenov *et al.*, The Fc-alpha receptor is a new target antigen for immunotherapy of myeloid leukemia. *Int. J. Cancer* **137**, 2729–2738 (2015).
57. A. M. Newman *et al.*, Robust enumeration of cell subsets from tissue expression profiles. *Nat. Methods* **12**, 453–457 (2015).
58. C. Woolsey, T. W. Geisbert, Current state of Ebola virus vaccines: A snapshot. *PLoS Pathog.* **17**, e1010078 (2021).
59. I. Martinez, L. L. Rodriguez, C. Jimenez, S. J. Pauszek, G. W. Wertz, Vesicular stomatitis virus glycoprotein is a determinant of pathogenesis in swine, a natural host. *J. Virol.* **77**, 8039–8047 (2003).
60. H. C. Aguilar *et al.*, N-glycans on Nipah virus fusion protein protect against neutralization but reduce membrane fusion and viral entry. *J. Virol.* **80**, 4878–4889 (2006).
61. C. T. Tan *et al.*, Relapsed and late-onset Nipah encephalitis. *Ann. Neurol.* **51**, 703–708 (2002).
62. C. E. Mire *et al.*, Recombinant vesicular stomatitis virus vaccine vectors expressing filovirus glycoproteins lack neurovirulence in nonhuman primates. *PLoS Negl. Trop. Dis.* **6**, e1567 (2012).

63. A. Marzi, F. Feldmann, T. W. Geisbert, H. Feldmann, D. Safronetz, Vesicular stomatitis virus-based vaccines against Lassa and Ebola viruses. *Emerg. Infect. Dis.* **21**, 305–307 (2015).
64. K. N. Bossart *et al.*, Receptor binding, fusion inhibition, and induction of cross-reactive neutralizing antibodies by a soluble G glycoprotein of Hendra virus. *J. Virol.* **79**, 6690–6702 (2005).
65. D. Pejoski *et al.*, Rapid dose-dependent natural killer (NK) cell modulation and cytokine responses following human rVSV-ZEBOV Ebolavirus vaccination. *NPJ Vaccines* **5**, 32 (2020).
66. C. Woolsey *et al.*, Immune correlates of postexposure vaccine protection against Marburg virus. *Sci. Rep.* **10**, 3071 (2020).
67. R. Elgueta *et al.*, Molecular mechanism and function of CD40/CD40L engagement in the immune system. *Immunol. Rev.* **229**, 152–172 (2009).
68. J. Willoughby, J. Griffiths, I. Tews, M. S. Cragg, OX40: Structure and function–What questions remain? *Mol. Immunol.* **83**, 13–22 (2017).
69. N. Isakov, A. Altman, Protein kinase C(θ) in T cell activation. *Annu. Rev. Immunol.* **20**, 761–794 (2002).
70. A. P. Huffman, J. H. Lin, S. I. Kim, K. T. Byrne, R. H. Vonderheide, CCL5 mediates CD40-driven CD4+ T cell tumor infiltration and immunity. *JCI Insight* **5**, e137263 (2020).
71. L. Li *et al.*, Ionic CD3-Lck interaction regulates the initiation of T-cell receptor signaling. *Proc. Natl. Acad. Sci. U.S.A.* **114**, E5891–E5899 (2017).
72. C. M. T. Freitas, D. K. Johnson, K. S. Weber, T cell calcium signaling regulation by the co-receptor CD5. *Int. J. Mol. Sci.* **19**, 1295 (2018).
73. Ö. Erdoğan *et al.*, Proteomic dissection of LPS-inducible, PHF8-dependent secretome reveals novel roles of PHF8 in TLR4-induced acute inflammation and T cell proliferation. *Sci. Rep.* **6**, 24833 (2016).
74. E. Quist-Paulsen *et al.*, High neopterin and IP-10 levels in cerebrospinal fluid are associated with neurotoxic tryptophan metabolites in acute central nervous system infections. *J. Neuroinflammation* **15**, 327 (2018).
75. C. Mathieu *et al.*, Lethal Nipah virus infection induces rapid overexpression of CXCL10. *PLoS One* **7**, e32157 (2012).
76. A. N. Prasad *et al.*, Resistance of cynomolgus monkeys to Nipah and Hendra virus disease is associated with cell-mediated and humoral immunity. *J. Infect. Dis.* **221**, S436–S447 (2020).
77. M. A. Whitt, Generation of VSV pseudotypes using recombinant ΔG-VSV for studies on virus entry, identification of entry inhibitors, and immune responses to vaccines. *J. Virol. Methods* **169**, 365–374 (2010).
78. S. M. Jones *et al.*, Live attenuated recombinant vaccine protects nonhuman primates against Ebola and Marburg viruses. *Nat. Med.* **11**, 786–790 (2005).
79. National Research Council, *Guide for the Care and Use of Laboratory Animals* (National Academies Press, Washington, DC, ed. 8, 2011).
80. C. Woolsey *et al.*, *Bundibugyo ebolavirus* survival is associated with early activation of adaptive immunity and reduced myeloid-derived suppressor cell signaling. *MBio* **12**, e0151721 (2021).